On the mechanics of edge cracking and the reliable determination of edge formability limits

On the mechanics of edge cracking and the reliable determination of edge formability limits

N Manopulo[1*], A R Chezan[2], E Atzema[2], I Picas Anfruns[2], B Carleer[3], J Pilthammar[4,5] and M Sigvant[4,5]

[1]AutoForm Development GmbH, Technoparkstrasse 1, 8005, Zurich, Switzerland
[2]Tata Steel, P.O. Box 10.000, 1970 CA Velsen-Noord, The Netherlands
[3]AutoForm Engineering Deutschland GmbH, Joseph-von-Fraunhofer-Straße 13a, 44227, Dortmund, Germany
[4]Volvo Cars, Dept. 81110 Strategy and Concept, 293 80 Olofström, Sweden
[5]Blekinge Institute of Technology, Valhallavägen, 371 41 Karlskrona, Sweden

*niko.manopulo@autoform.ch

Abstract. Blanked edge surfaces are rough and hardened. They therefore lead to inhomogeneous deformation on the edge, which can trigger localization within the shear affected zone (up to few mm from the edge). The size and extent of these phenomena are primarily a function of the shearing process and are only marginally coupled to the global/homogeneous deformation behavior of the blank. A direct numerical simulation of such local deformation effects would require a prohibitively high resolution to capture the microgeometry of the edge and thus remains unfeasible in the current industrial practice. A predictive model can therefore only be achieved by determining limit strains on the edge, which are compatible with the homogeneous numerical framework used. The present contribution aims discussing the basic mechanics of edge cracking based on tensile tests with edges blanked with different die clearances. The local and global strain evolutions in the vicinity of the edge are analysed and a new evaluation procedure is proposed for the reliable determination of limit strains. The application of this method in industrial context is also discussed.

1. Introduction

The most common failure mode in stamping operations is splitting due to localized necking. The stress / strain states triggering necking, naturally arise during deformation and therefore usually span a macroscopic extent of the stamped parts. This means that once necking sets in, it almost immediately develops into a global instability and cracks. It is therefore reasonable to set the failure limit at the onset of localized necking (FLC), which in turn is also compatible with the state of the art numerical framework based on shell elements and continuum mechanics. However, in case of edge cracking the necking initiation occurs in a strongly confined region, whereas the global deformation remains stable. It is therefore more challenging to find a deformation limit which adequately represents the fracture phenomenon but at the same time remains compatible with state of the art numerical computation results. Edge crack prediction, especially in case of particularly sensitive materials such as DP steels and AA6xxx alloys, has attracted significant scientific attention in the recent years. A large number of different experimental designs with similarly many evaluation approaches have been proposed. Differently than in other occasions, the scientific efforts have not converged towards a simple standardized set of experiments for direct application in industrial practice. An exhaustive review of the available experiments lies outside the scope of this work and is in any case a real challenge. However,

three different categories can be recognized: tensile tension tests, hole expansion tests and edge extension tests. Examples in the first category are approaches based on a simple tensile geometry such as in [1] or [2]. Although these can be evaluated directly, they are also mostly coupled to DIC based strain measurements. Hole expansion tests of flat and conical type are also very popular also thanks to partial standardization (see e.g. [3]). Finally alternative approaches exist such as the Diabolo test [5][6] and improvements thereof [7] or completely new geometries [8].

All of the mentioned approaches use different evaluation procedures which results in a large scatter of limit strains even for the same material grades. As also recognized in [7], this is only one side of the coin. In fact, the important question of whether the evaluation methods are compatible with numerical computations still remains not thoroughly studied. The present contribution aims taking a step in this direction and propose a new evaluation method based on DIC measurements, which takes into account the length scale compatibility between reality and simulation.

2. Materials characterization

The sheets used in this study are CR440Y780T-DP (referred to as DP800) with a thickness of 1.5mm provided by Tata Steel and the HyperForm™ variation of the same grade CR440Y780T-DH (referred to as DH800). The basic mechanical properties of the materials can be found in Table 1

Table 1. Mechanical Properties DP800

Material	A_g [%]	R_m [MPa]	σ_0 [MPa]	σ_{45} [MPa]	σ_{90} [MPa]	r_0 [-]	r_{45} [-]	r_{90} [-]
DP800	12.5	827.6	490.1	488.1	496.5	0.75	0.85	0.875
DH800	15.6	798.8	404.3	404.7	407.5	0.81	0.85	1.018

For the AutoForm™ simulations in the following chapters, material models provided by Tata Steel™ in the AutoForm™ database have been used. These provide a strain rate dependent flow curve description in tabular form, the Vegter 2017 yield locus description [9] as well as an FLC calculated according to [10]. Figure 1 provides a comparison of the two material models used. For a more detailed description of these data and models the reader is referred to the AutoForm Material Database and to the corresponding publications.

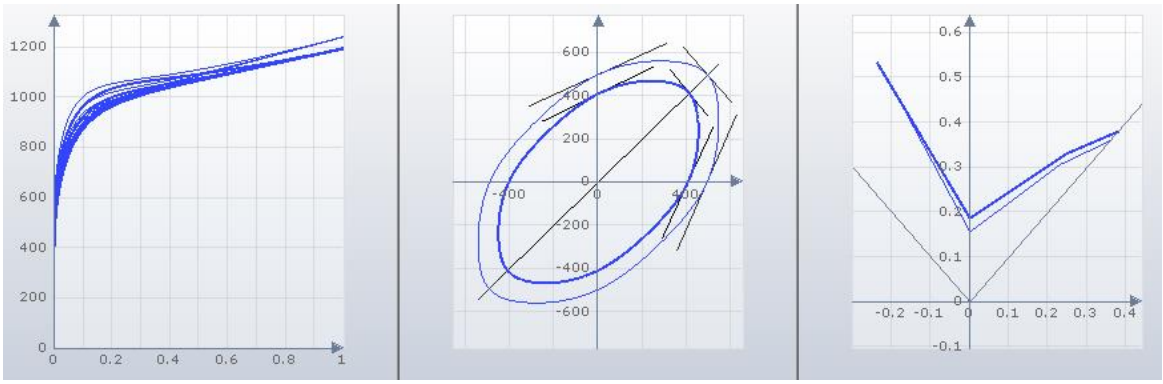

Figure 1. Material models for DP800 (thin lines) and DH800 (thick lines)

3. Edge cracking tensile test

The SETi tests have been chosen for this study as proposed by [1]. Rectangular specimens of 20 mm width have been blanked out of the sheet using different tool clearances. The specimens have subsequently been clamped in a tensile machine with an unsupported length of 50 mm and drawn until fracture. The deformation field has been captured using the GOM™ Aramis system.

Table 2. Average true strains at fracture for different clearances

Clearance	3%	15%	25%
DP800	0.12	0.18	0.19
DH800	0.16	0.18	0.19

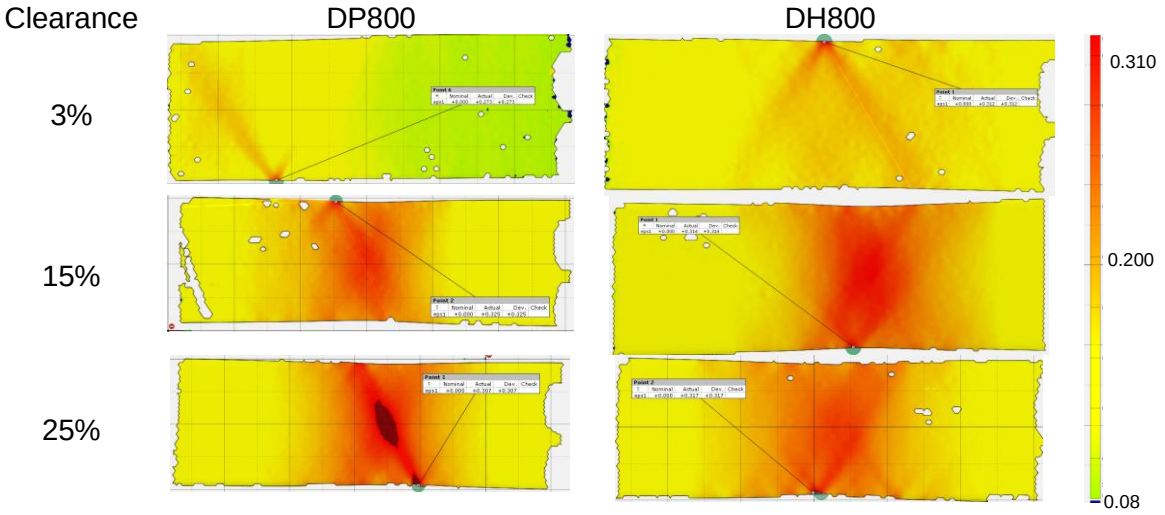

Figure 2. GOM Aramis major principal strain fields for different clearances

Table 2 depicts the average true strain computed from the GOM Aramis data using a virtual extensometer with 45mm gage length. It is qualitatively observed that an increase in clearance is beneficial to the global formability. Additionally, it is seen that the DH800 also provides superior edge formability especially in the critical low clearance case. However, using these values quantitatively, as limiting strains for stamping simulations, would clearly be too conservative. In fact, looking at Fig 2, it is seen that right before crack initiation the specimen already started building macroscopic shear bands. On the other hand, looking at the local true strains at the critical points right before fracture we obtain values around 0.31 for all specimens (see Table 3).

Table 3. Local true strains at fracture at the critical point for different clearances

Clearance	3%	15%	25%
DP800	0.27	0.33	0.31
DH800	0.31	0.31	0.32

Having a nearly constant local strain at fracture should not be surprising. In fact this simply shows that at a strain of about 0.31 on the edge the load carrying capacity of the material is lost. However, depending on the edge condition this value is reached more or less quickly, thus creating significant differences in the corresponding global deformations, which in turn are the important measures for use together with simulations. It is therefore necessary to separate the influence of the edge deformation from the natural/global deformation of the specimen.

Fig. 3 helps understanding the causes of these strong differences in edge formability. In fact it is noted that the 3% clearance delivers a more homogeneous surface with less die roll, whereas the 25% clearance fails abruptly in shear mode at roughly 1/3 of the initial thickness and features a higher die roll. At first sight this might sound counter-intuitive, given that the small clearance delivers a sharper or “better” edge surface. However, it should be considered that this better surface quality is achieved because the material separates only after significant plastic deformation, which partially depletes the formability of the material in the near (macroscopic) vicinity of the edge. In contrast in the large clearance case, plastic deformation only occurs in roughly 1/3 of the thickness. The rest of the section is fractured abruptly, thus affecting only a microscopic vicinity of the edge. As a consequence the small clearance case

delivers stronger differences in hardness between edge and interior, leading to a faster development of necks on the edge.
This fact should, however, not be interpreted as a generic advantage of using large clearances for trimming. In fact the abrupt nature of the fracture in the large clearance case also means that the outcome will be more unstable or less repeatable than the small clearance case. This point will be discussed more in detail in Section 6.

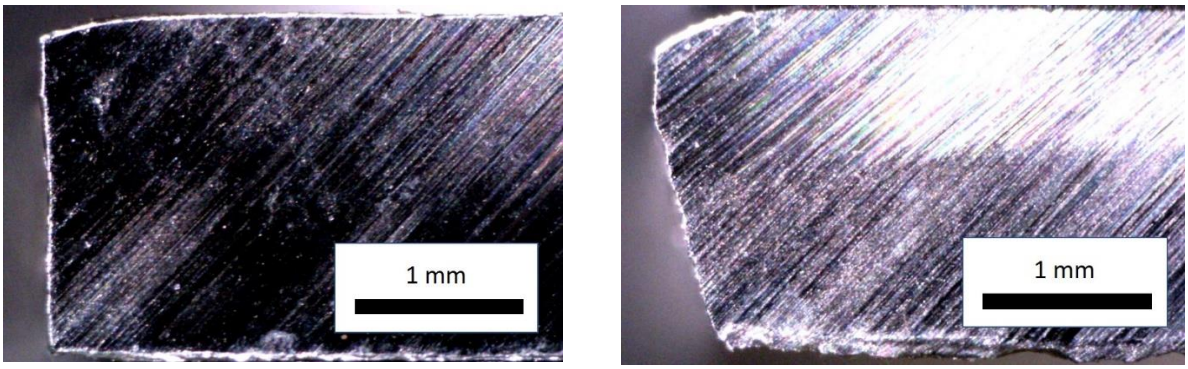

Figure 3. Comparison of blanked SETi specimens with 3% (left) and 25% die clearance

4. A new evaluation method for reliable edge formability prediction

As mentioned in the previous paragraphs the central question revolves about distinguishing between local and global deformations. A discussion of localization and length scales will therefore be made first in order to elucidate the rationale behind the approach. The concrete steps and the evaluated results will be given in the following.

4.1. Necking, length scales and mesh size dependency

Localized necking occurs when the strains can no longer be effectively distributed in the sheet plane and thickness reduction is the only remaining plasticity mechanism before fracture. As such, localized necking is a negative feedback loop meaning that thinning results in stronger localization of strains, which in turn induce stronger thinning. This means, once initiated, strain rates show exponential growth and necking region becomes correspondingly narrow. The local strain within the neck is therefore very sensitive and can get arbitrarily high values depending on the resolution of the evaluation method. Due to this dependency to a length scale, local strains have low reliability.
The problem of size dependency in negative feedback processes is well studied in the literature of coupled damage accumulation processes. The remedy commonly resorted to is the definition of the significant quantities using a non-local formulation. In this approach the quantities are defined not directly in terms of the local values but as a function of the neighbouring values as well, within a length scale independent of the mesh size. This makes sure that the computed data are primarily a function of the defined length scale and not of the mesh size which may be arbitrary.
The definition of a nonlocal counterpart q for any relevant quantity q can be achieved using the following formulation:

$$\bar{q}(x) = \frac{\int_\Omega w(x-a)q(a)da}{\int_\Omega w(x-a)da} \quad (1)$$

Please note that this simply corresponds to a filtering of the local values using a weighting function w and within the bounds of a region described by the length scale parameter a.
Digital image correlation methods evaluate strains based on a discrete grid and therefore local strains in necked regions also suffer a dependency on the resolution (facet size). So a low resolution delivers lower strains in the neck and vice versa. A robust evaluation of the strains in a DIC results needs to be defined in terms of a length scale which is independent of the resolution. The latter should also be chosen at a similar scale to the FEM element size in order to ensure compatibility to numerical results.
The next question is the definition of a meaningful and compatible length scale in the context of detecting necking initiation of metallic sheets. The macroscopic extent of a local neck is often reported

to roughly correlate to the sheet thickness (e.g. in M-K model). Therefore the blank thickness can be considered a good scale to describe the global strains in the neck. For the material under consideration, the thickness is 1.5mm which is also in the same ballpark as the ideal mesh size for adaptively refined regions in numerical simulations for most automotive applications.

4.2. Description of the evaluation method

4.2.1. STEP 1: Identification of the Crackpoint. The first step in the evaluation is the identification of the edge point at which crack initiation is detected (P_i). To do this, the last picture before the appearance of a visible crack is selected, and the point with highest major strain is marked (Figure 4, left). Both the major strain and the thickness strain rate are evaluated over the whole history at this point.

4.2.2. STEP 2: Definition of the influence region. Next a circle with diameter equal to the blank thickness is defined centered on P_i and the minimal amount of surface facets completely containing the circle are selected and grouped (Figure 4, right). Both the major strain and the thickness strain rate are evaluated over the whole history at this point as averages over the defined region.

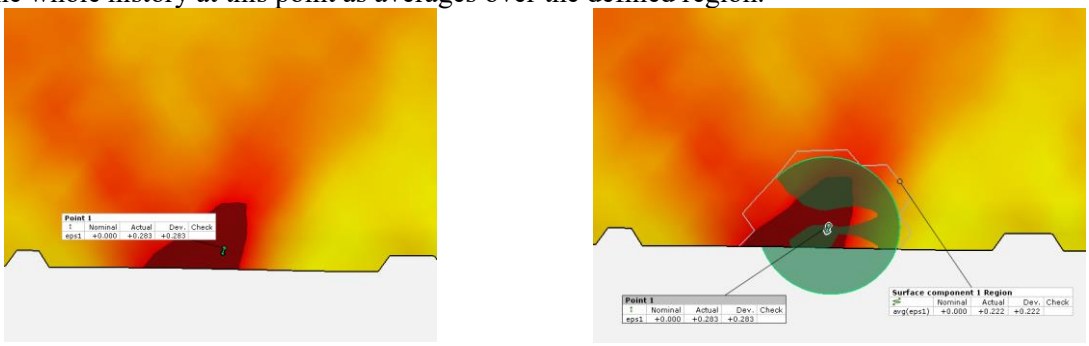

Figure 4. Selection of crack initiation point (left) and definition of influence region (right)

4.2.3. STEP 3: Identification of necking initiation time. Figure 5 depicts respectively the major strain (left) and the thickness strain rate (right) for both the local and the averaged quantities. It can be seen that the averaged quantities function as stable estimators of the local quantities throughout the uniform deformation. When localized necking kicks in, the local thickness strain rate grows exponentially whereas the averaged strain rate remains as expected stable. So localized necking is defined to begin when the difference between local and averaged strain rates exceeds the natural scatter in the local thickness strain rate. The latter is measured by the Median Absolute Deviation (MAD). This condition can be formulated by the following expression

$$I_{neck} = \text{index}\left[\, \left|\dot{\varepsilon}_{3,loc} - \dot{\varepsilon}_{3,avg}\right| > MAD\left(\dot{\varepsilon}_{3,loc}\right)\right] \quad (2)$$

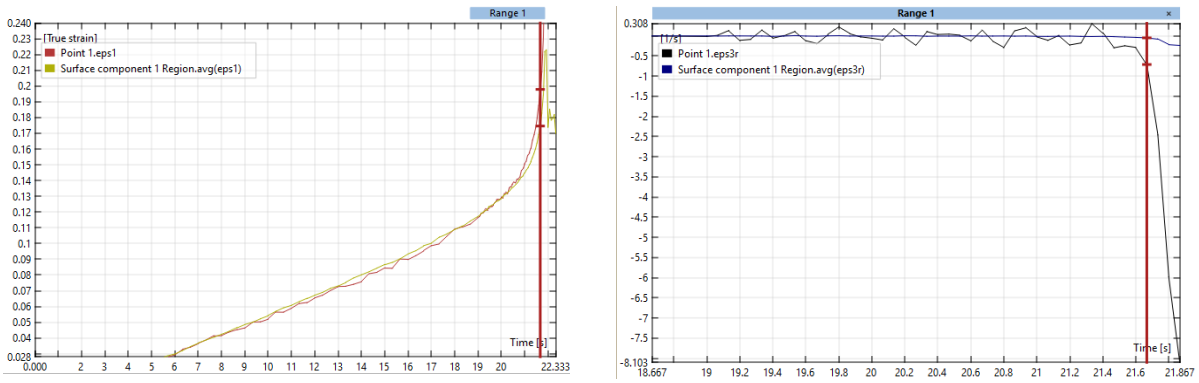

Figure 5. Evolution of local and averaged major strains (left) and evolution of local and averaged thickness strain rates zoomed at a time range close to necking (right)

4.2.4. STEP 4: Evaluation of nonlocal major strain limit. A nonlocal scheme of the form introduced in Eq. 1 can be easily constructed with any weighting function, if detailed access to topology and point data is available from the DIC. A simple but effective approach is proposed at this stage only relying on the data computed in the previous steps which essentially approaches the behavior of a gauss filter. The limiting strain is thus defined as follows:

$$\varepsilon_{1,limit} = \alpha\, \varepsilon_{1,local} + (1-\alpha)\varepsilon_{1,avg} \quad (3)$$

The local strain is less reliable than the locally averaged strain, it is therefore recommended to set the mixing factor at α=0.25. Please note that this formula essentially corresponds to choosing the following weighting function in eq. 1:

$$w(x-a) = \alpha\delta(x-x_c) + (1-\alpha) \quad (4)$$

where $\delta(x-x_c)$ is the delta Dirac function to filter out the local strain at the center $x_c$of the definition circle, whereas the constant 1 represents the averaging operator. The weighting function w is constant with respect to the length scale a**,** which however comes in the picture with the definition of the domain for the averaging (integral).

4.3. Evaluation of SETi Tests

Table 4 depicts the evaluated SETi tests for the two materials. The DP800 material shows a monotonously increasing trend with increasing clearance, whereas the DH800 shows more scatter but also an overall better edge formability.

Table 4. Nonlocal true strain at edge fracture

Clearance	3%	15%	25%
DP800	0.19	0.24	0.26
DH800	0.22	0.28	0.25

5. Interpretation of the results and industrial application

The following two interpretations can be made based on the mentioned results:

1. A clearance of about 15% to 25% is optimal for this material and should be implemented wherever possible. If the corresponding strain limit is exceeded in the simulation, it means that edge cracks would most probably appear in tryout and will likely not be fixable only by influencing the tool arrangement. It is advisable to fix the problem at the design stage.
2. The minimum value measured is 0.19. If any region along the trimming contour exceeds this value, there will be a potential risk in tryout depending on the real clearance of the tools. If the position of the spot is not vital or is easy to fix in tryout, the solution of this issue can be deferred to tryout, with the recommendation of controlling the local clearance of the tools.

Any strain levels below the 0.19 strain level should be considered safe. If such spots fail in tryout this should be indicative of either an excessively small (low residual formability) or excessively large (high uncertainty in edge condition) clearance.

5.1. Application to a real example

The evaluated limits have been applied on a part design provided by Volvo Cars. The edge crack limits in AutoForm have been defined as follows:

Table 5. Edge Crack Limits in AutoForm

Edge Condition	**Laser Cut**	**Sharp Steel**	**Worn Steel**
Limit Strain [-]	0.32	0.26	0.19

Where the laser cut limit corresponds to the maximum local value measured in the experiments, the worn steel value has been taken from 3% clearance and sharp steel value corresponds to 25% clearance. The simulation results depicted in Fig. 7 suggest a single critical spot in position A, which is however critical for all three edge condition classes. There is a strain peak also in position B, but this remains subcritical. Comparing this prediction to tryout results we observe two crack spots, one in position A, as expected, but also a crack in position B, which should have been safe.

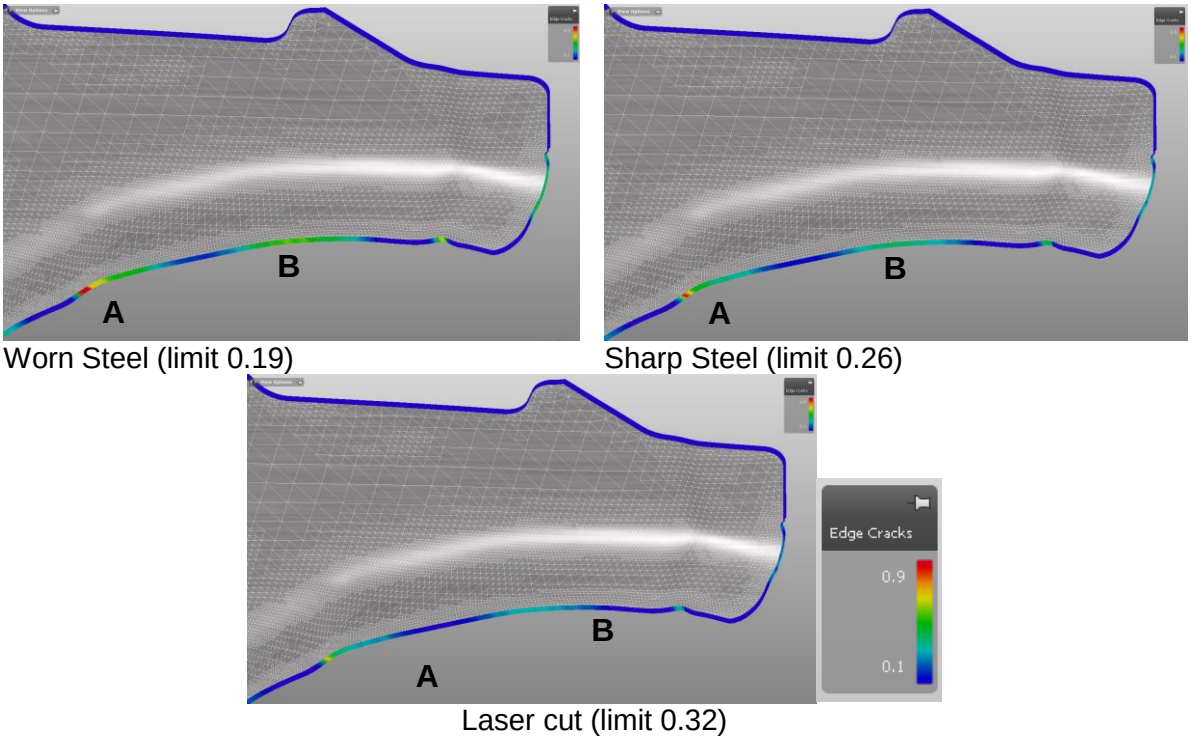

Figure 6. Edge Crack failure values in AutoForm for the industrial part provided by Volvo Cars with worn steel (above left) sharp steel (above right) and laser cut (below) values

A deeper look on the edge conditions at these spots (Figure 7) gives better insight on the mechanisms that caused the fractures. In fact it is clear that the effective clearance in spot A has been relatively low, in the ballpark of 3% making this spot very critical as also predicted by the simulation. Spot B on the other hand featured a very large effective clearance, probably significantly higher than the measured maximum of 25%. In this case it is seen that the problem is not directly due to the clearance effect itself but indirectly due to the unstable fracture mechanism caused by the excessive clearance. In fact, Figure 7 (right) shows a cup-cone type separation of the material in the trimming stage, which significantly reduces the section area actively carrying the tensile load on the edge.

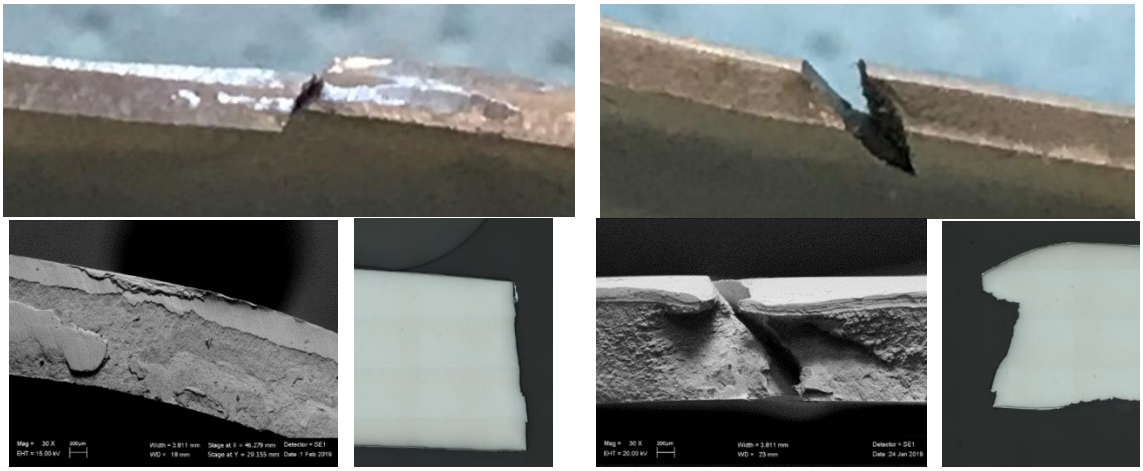

Figure 7. Edge conditions in spot A (left) and spot B (right)

6. Conclusions

The topic of experimental/numerical compatibility has been the central theme of this contribution. Further studies are necessary to completely exhaust the topic especially regarding issues related to time resolution of the experiments and quantitative assessment of experimental robustness. The following recommendations can be drawn from the conducted study:

- Standardization in the execution and evaluation of edge fracture experiments is of central importance in achieving predictive simulation results. Special care needs to be taken to ensure compatibility between experiments and numerical simulations.
- Experimental approaches should cover a possibly wide range of process conditions (clearances, tool radii etc.) and consequentially the simulations must be evaluated for different scenarios related to process conditions
- Due to the rich variety of conditions encountered in real tools, a residual uncertainty is nowadays unavoidable, even if the material behavior is robustly characterized. The engineering effort should therefore not be limited to predicting possible edge cracks, but also design possible remedies depending on the actual conditions in the tryout press.

7. References

[1] Atzema E and Seda P 2015 *Proc. of FTF 2015 Zürich Switzerland*
[2] Feistle M, Golle R and Volk W 2015 *Proc. of 48th CIRP Conf.*
[3] ISO 16630 2009. *ISO copyright office, Geneva, Switzerland*
[4] VDI 3359 2013 *Association of Engineers, Beuth Verlag GmbH, Düsseldorf*
[5] Wiegand K 2016 *Proc. of IDDRG 2016, Graz, Austria*
[6] Liewald M and Gall M 2013 *Proc. of IDDRG 2013, Zurich, Switzerland*
[7] Sigvant M, Falk J and Pilthammar J 2017 *J Phys: Conf. Ser.* **896** 012101
[8] Larour P, Schauer H, Lackner J and Till, E 2016 *Proc. of IDDRG 2016, Graz, Austria*
[9] Abspoel M, Scholting M E, Lansbergen M, An Y, Vegter H 2017 *J Mater Process Technol.* **248** 161-177
[10] Abspoel M, Scholting M E, Droog J M 2013 *J Mater Process Technol.* **213** 759–769.